

Temperature dependence of the damping parameter in the ferrimagnet $\text{Gd}_3\text{Fe}_5\text{O}_{12}$

Isaac Ng,^{1,2 a)} Ruizi Liu^{1,3 a)}, Zheyu Ren^{1,3}, Se Kwon Kim,⁴ and Qiming Shao^{1,2,3 b)}

¹*Department of Electronic and Computer Engineering Department, Hong Kong University of Science and Technology, Clear Water Bay, Kowloon, Hong Kong SAR, China*

²*Department of Physics, Hong Kong University of Science and Technology, Clear Water Bay, Kowloon, Hong Kong SAR, China*

³*Guangdong-Hong Kong-Macao Joint Laboratory for Intelligent Micro-Nano Optoelectronic Technology, The Hong Kong University of Science and Technology, Hong Kong, China*

⁴*Department of Physics, Korea Advanced Institute of Science and Technology, Daejeon 34141, Republic of Korea*

^{a)} Contributed equally ^{b)} Email: eeqshao@ust.hk

Abstract

The damping parameter α_{FM} in ferrimagnets defined according to the conventional practice for ferromagnets is known to be strongly temperature dependent and diverge at the angular momentum compensation temperature, where the net angular momentum vanishes. However, recent theoretical and experimental developments on ferrimagnetic metals suggest that the damping parameter can be defined in such a way, which we denote by α_{FiM} , that it is free of the diverging anomaly at the angular momentum compensation point and is little dependent on temperature. To further understand the temperature dependence of the damping parameter in ferrimagnets, we analyze several data sets from literature for a ferrimagnetic insulator, gadolinium iron garnet, by using the two different definitions of the damping parameter. Using two methods to estimate the individual sublattice magnetizations, which yield results consistent with each other, we found that in all the used data sets, the damping parameter α_{FiM} does not increase at the angular compensation temperature and shows no anomaly whereas the conventionally defined α_{FM} is strongly dependent on the temperature.

Antiferromagnets have been one important focus in spintronics due to their properties distinct from more conventional ferromagnets including the zero stray field, ultrafast dynamics, and immunity to external field^{1,2}. Recently, antiferromagnetically coupled ferrimagnets have emerged as a new material platform to study antiferromagnetic dynamics as suggested by the recent discoveries of current-driven magnetization switching near magnetization compensation point^{3,4}, where the net magnetization vanishes, and fast domain-wall dynamics at the angular momentum compensation temperature^{4,5,6,7}, where the net angular momentum vanishes. However, magnetic resonance and dynamics of ferrimagnets have not been fully understood partly due to the involvement of multiple magnetic sublattices and the resultant internal complexity. The dissipation rate of angular momentum in magnetic material is manifested as the linewidth in resonance spectrum. One quantity of particular importance in the dissipative dynamics of ferrimagnets is the damping parameter, which is a characteristic of the magnetic material that determines the Gilbert-like damping of angular momentum and is usually denoted by the dimensionless number α . Early literature suggested that the effective damping parameter α_{FM} for ferrimagnets defined by a value that is proportional to the linewidth of the resonance response is strongly temperature-dependent and increases anomalously near the angular momentum compensation temperature (T_A).⁸ Recent studies have provided a new interpretation: the damping parameter can be defined in such a way that it is independent of temperature near the T_A while the temperature dependence of the ferromagnetic resonance (FMR) is attributed to the temperature dependence of the net angular momentum.^{9,10,11} A. Kamra *et al.* have theoretically demonstrated this new perspective by accounting the Rayleigh dissipation function in a two-sublattice magnetic system, and the resultant Gilbert damping parameter is independent of temperature near the T_A .¹¹ This damping parameter denoted by α_{FiM} is defined as follows:

$$\alpha_{\text{FiM}} = \left| \frac{s_{\text{net}}}{s_{\text{total}}} \right| \alpha_{\text{FM}}, \quad (1)$$

where the s_{net} and s_{total} are the net and total angular momentum, respectively. The s_{net} is calculated by the difference of the angular momentum between two sublattices ($s_{\text{net}} = |s_1 - s_2|$) and s_{total} is calculated by the total magnitude of the angular momentum ($s_{\text{total}} = |s_1| + |s_2|$). D.-H. Kim *et al.* have experimentally studied the current-driven domain wall motion in ferrimagnetic metal alloy GdFeCo and revealed that the damping parameter α_{FiM} is indeed independent of temperature near the T_A .¹⁰ Furthermore, T. Okuno *et al.* has reported that α_{FiM} of the GdFeCo is temperature

independent when the FMR measurement temperature is approaching the T_A .⁶ The FMR of ferrimagnetic thin films below the T_A is difficult to achieve because of much enhanced perpendicular magnetic anisotropy at lower temperatures. It would be desirable that a full temperature range of FMR can be investigated for ferrimagnets.

The divergence of the conventionally defined damping parameter α_{FM} at T_A can be understood easily by considering the energy dissipation rate given by $P = \alpha_{\text{FM}} s_{\text{net}} \dot{\mathbf{m}}^2$ (which is twice the Rayleigh dissipation function), where \mathbf{m} is the unit magnetization vector. For the given power P that is pumped into the ferrimagnet by e.g., applying microwave for FMR, as the temperature approaches T_A , the net spin density s_{net} decreases and thus α_{FM} increases. Exactly at T_A , the net spin density vanishes, making α_{FM} diverge and thus ill-defined. Note that the divergence of α_{FM} at T_A is due to the appearance of the net spin density s_{net} in the dissipation rate and should not be interpreted to indicate the divergence of the dissipation rate, which is always finite. In terms of the alternative damping parameter α_{FiM} , the energy dissipation rate is given by $P = \alpha_{\text{FiM}} s_{\text{tot}} \dot{\mathbf{m}}^2$. The total spin density s_{tot} is always finite and has weak temperature dependence, and thus α_{FiM} is well-defined at all temperatures with possibly weak temperature dependence. This suggests that α_{FiM} , which is well-defined at all temperatures, might be more useful to describe the damping of ferrimagnetic dynamics, particularly in the vicinity of T_A , than the more conventional α_{FM} which diverges and thus ill-defined at T_A . One way to appreciate the physical meaning of α_{FiM} is to consider a special model, where the energy dissipation of a ferrimagnet occurs independently through the dynamics of each sublattice and all the sublattices have the same damping parameter. In this case, α_{FiM} is nothing but the damping parameter of the sublattices. So far, the discussion of ferrimagnetic damping is limited to ferrimagnetic metals, while ferrimagnetic insulators have shown the potential for ultralow-power spintronics.^{12,13,14,15,16}

In this paper, we investigate the temperature dependence of damping parameters in ferrimagnetic insulator, gadolinium iron garnet ($\text{Gd}_3\text{Fe}_5\text{O}_{12}$, GdIG), by surveying the literature of studies on the temperature dependence of FMR. Since the s_{total} is usually not given in the literature, we adopt two different methods to calculate the individual sublattice magnetization (M_{Fe} and M_{Gd}) and then evaluate s_{total} . The first method is to use the magnetization of yttrium iron garnet ($\text{Y}_3\text{Fe}_5\text{O}_{12}$, YIG) as the M_{Fe} as done in Ref.¹⁷, where nuclear magnetic resonance experiments show that the magnetization contribution from iron is similar in YIG and GdIG since yttrium does not contribute the magnetization in YIG, and then obtain M_{Gd} from the net magnetization and M_{Fe} . The second

method uses Brillouin-like function to simulate the temperature dependence of GdIG magnetization, the angular momentum of each individual sublattice can be calculated with the Brillouin function. We found consistent results between these two different methods that the damping parameter α_{FiM} is almost temperature-independent near the T_A , unlike the conventionally defined α_{FM} which is strongly temperature-dependent and diverge at T_A .

The FMR linewidth (ΔH) of GdIG is utilized to find the conventional damping parameter α_{FM} :

$$\Delta H = \frac{\alpha_{\text{FM}}}{g_{\text{eff}} \mu_B / \hbar} f_{\text{res}} + \Delta H_0, \quad (2)$$

where g_{eff} is the effective Landé g-factor, μ_B is the Bohr magneton, \hbar is the reduced Planck constant, ΔH_0 is the frequency-independent inhomogeneous broadening linewidth, and f_{res} is the resonance frequency. Then, to convert the α_{FM} to the α_{FiM} , we need to find the ratio $\frac{s_{\text{net}}}{s_{\text{total}}}$. Note that α_{FM} diverges as the temperature approaches T_A , meaning that Eq. (2) can be used only when it is sufficiently far away from the T_A . Therefore, we will only employ data sufficiently far away from T_A in this perspective. The net spin density s_{net} is calculated from the difference between the angular momentum of Fe and Gd:

$$\begin{aligned} s_{\text{Fe}} &= \frac{M_{\text{Fe}}}{g_{\text{Fe}} \mu_B / \hbar}, \\ s_{\text{Gd}} &= \frac{M_{\text{Gd}}}{g_{\text{Gd}} \mu_B / \hbar}, \\ s_{\text{net}} &= |s_{\text{Fe}} - s_{\text{Gd}}| = \frac{M_{\text{net}}}{g_{\text{eff}} \mu_B / \hbar}, \end{aligned} \quad (3)$$

where the M_{net} is the net magnetization, g_{Fe} and g_{Gd} is the Landé g-factor of the iron and gadolinium sublattice, respectively. The net magnetization is given by

$$M_{\text{net}} = |M_{\text{Fe}} - M_{\text{Gd}}|, \quad (4)$$

which is normally measured by a superconducting quantum interference device or a vibrating-sample magnetometer and provided in the literature.^{18,19,20}

METHOD 1

We can use the magnetization of YIG as an approximation for the M_{Fe} to calculate the M_{Fe} and M_{Gd} from GdIG net magnetization, as yttrium does not contribute to the magnetization of YIG, which we refer to as *Method 1*. Experimentally, Boyd *et al.*¹⁷ used the nuclear ferromagnetic

resonance technique to determine temperature-dependent M_{Fe} in YIG and GdIG and found that they are very similar. This approximation has been used in previous literature and has produced reasonable results.²¹ The magnetization of YIG is obtained from Ref.18. With M_{Fe} and M_{Gd} known, we can determine the angular momentum of each sublattice with its respective g-factor. The g factors of Fe and Gd are very similar, the g-factor of iron is measured from YIG and is determined as $g_{Fe} = 2.0047$.²² The g-factor of Gd sublattice is $g_{Gd} = 1.994$ and is determined by measurement of GdIG²³. The T_M and T_A will be very close to each other, with T_A slightly higher than T_M . We can calculate the total spin density s_{total} using

$$s_{total} = s_{Fe} + s_{Gd} . \quad (5)$$

The net spin density s_{net} can be calculated using Eq. (3) and we can obtain effective g-factor meanwhile. Finally, we can calculate the α_{FM} using Eq. (2) and the α_{FiM} using Eq. (1).

METHOD 2

The second method is to use the Brillouin-like function to simulate the temperature dependence of magnetization.²⁴ Due to the weak coupling of the Gd-Gd interaction, the gadolinium magnetic moments follow a paramagnetic behavior and increase drastically at low temperatures. The net magnetization in GdIG can be described by the sum of the three sublattices with a and d sublattices corresponding to Fe and c sublattice corresponding to Gd:

$$M_{net} = |M_a + M_c - M_d| . \quad (6)$$

The individual magnetization component can be simulated by the Brillouin function $B_{S_i}(x_i)$

$$M_i(T) = M_i(0)B_{S_i}(x_i) . \quad (7)$$

The $M_i(0)$ is the individual magnetization at 0 K.

$$\begin{aligned} M_d(0) &= 3n_{m_{Fe}} = 3ng_d S_d \mu_B , \\ M_a(0) &= 2n_{m_{Fe}} = 2ng_a S_a \mu_B , \\ M_c(0) &= 3n_{m_{Gd}} = 3ng_c S_c \mu_B , \end{aligned} \quad (8)$$

n is the number of GdIG formula unit per unit volume, it can be calculated using $N_A/(\rho M_r)$, where N_A is the Avogadro's number, ρ and M_r are the density (6.45 gcm^{-3} ²⁵) and molar mass (942.97)

of GdIG respectively. S_i is the electron spin of the respective sublattice. For GdIG, S_d and S_a are 5/2 and S_c is 7/2. g_i is the individual g factor and x_i is defined as:

$$\begin{aligned} x_d &= \left(\frac{\mu_0 S_d g_d \mu_B}{k_B T} \right) (n_{dd} M_d + n_{da} M_a + n_{dc} M_c), \\ x_a &= \left(\frac{\mu_0 S_a g_a \mu_B}{k_B T} \right) (n_{ad} M_d + n_{aa} M_a + n_{ac} M_c), \\ x_c &= \left(\frac{\mu_0 S_c g_c \mu_B}{k_B T} \right) (n_{cd} M_d + n_{ca} M_a + n_{cc} M_c), \end{aligned} \quad (9)$$

n_{ij} are the Weiss coefficients between two sublattices, which account for the intersublattice molecular field coupling ($i \neq j$) or intrasublattice molecular field interactions ($i = j$).²⁴ μ_0 is permeability of vacuum.

To determine the s_{net} and s_{total} from the magnetization fitting will require the sublattice g-factor g_{Gd} and g_{Fe} . g_{Fe} in a and d sublattice can be experimentally measured from YIG and is determined as $g_{\text{Fe,d}} = 2.0047$, $g_{\text{Fe,a}} = 2.003$.²² The g-factor of Gd c sublattice has the same value as the one in Method 1, $g_{\text{Gd}} = 1.994$.²³ With the value of the individual sublattice g-factor, the angular momentum of each sublattice can be calculated from Eq. (3). Then we can calculate the effective gyromagnetic ratio and effective g-factor with the sublattice magnetization and angular momentum.

$$\begin{aligned} \gamma_{\text{eff}} &= \frac{M_{\text{Fe,d}} - M_{\text{Fe,a}} - M_{\text{Gd,c}}}{S_{\text{Fe,d}} - S_{\text{Fe,a}} - S_{\text{Gd,c}}}, \\ g_{\text{eff}} &= \frac{\gamma_{\text{eff}} \hbar}{\mu_B}, \end{aligned} \quad (11)$$

The ratio $s_{\text{net}}/s_{\text{total}}$ can be calculated where $s_{\text{net}} = |S_{\text{Fe,d}} - S_{\text{Fe,a}} - S_{\text{Gd,c}}|$ and $s_{\text{total}} = S_{\text{Fe,d}} + S_{\text{Fe,a}} + S_{\text{Gd,c}}$, with both the g_{eff} and angular momentum known. Eventually, the value of α_{FiM} is obtained from Eq. (1).

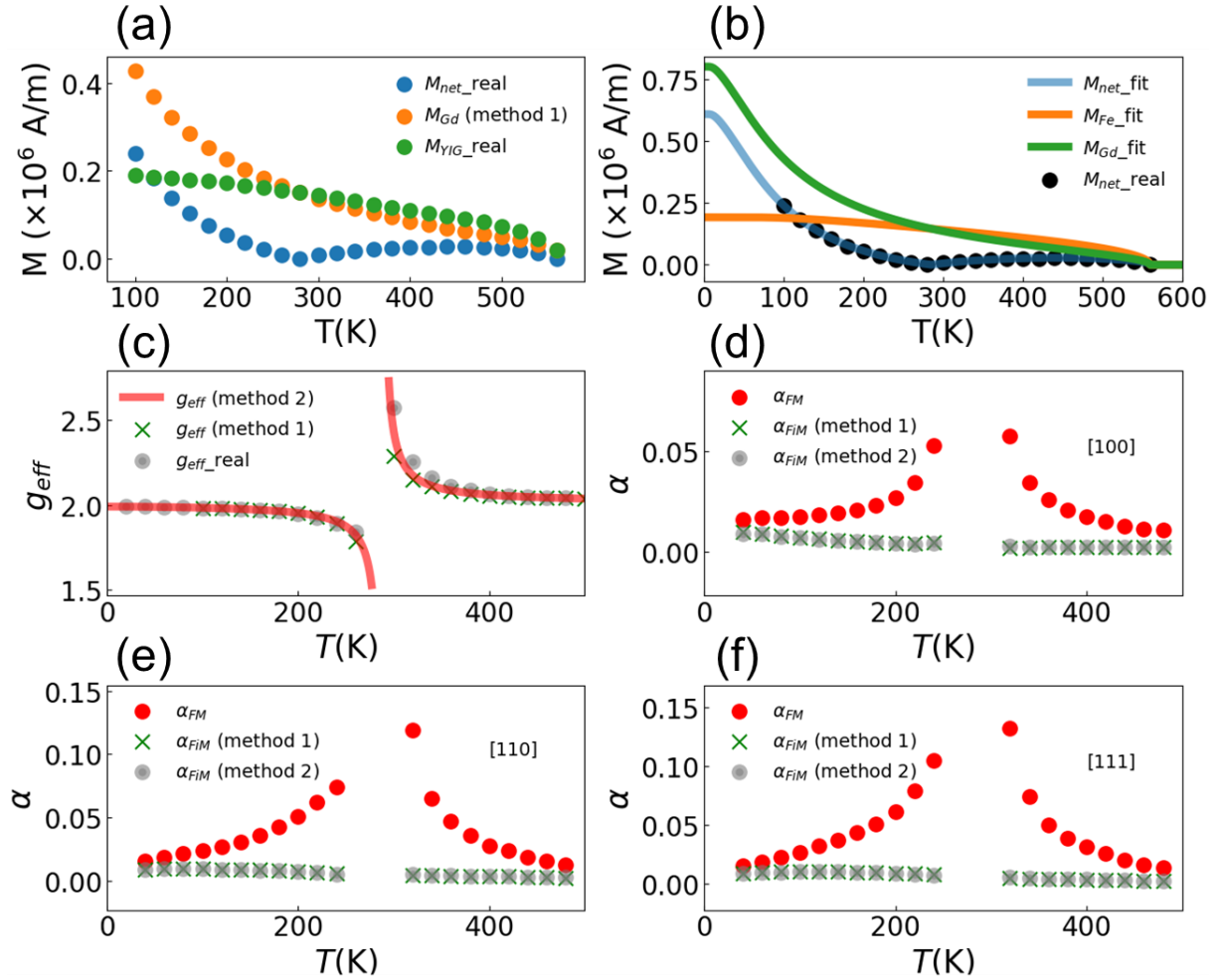


Figure 1. The analysis of GdIG data from Rodrigue *et al.*²³ and Dionne *et al.*¹⁸ (a) Calculated individual magnetization as a function of temperature using Method 1. (b) The Magnetization curve of GdIG using Brillouin fitting method (Method 2) compared to the magnetization from Dionne *et al.*¹⁸ (c) The g_{eff} of GdIG calculated from Method 1 as the green cross and from Method 2 as the red line compared to the grey dot g_{eff} from Rodrigue *et al.* ([100] direction).²³ (d) (e) (f) Comparing the damping parameter α_{FM} (red dot) to α_{FiM} based on Method 1 (green cross) and α_{FiM} based on Method 2 (grey dot) for three directions ([100], [110] and [111]).

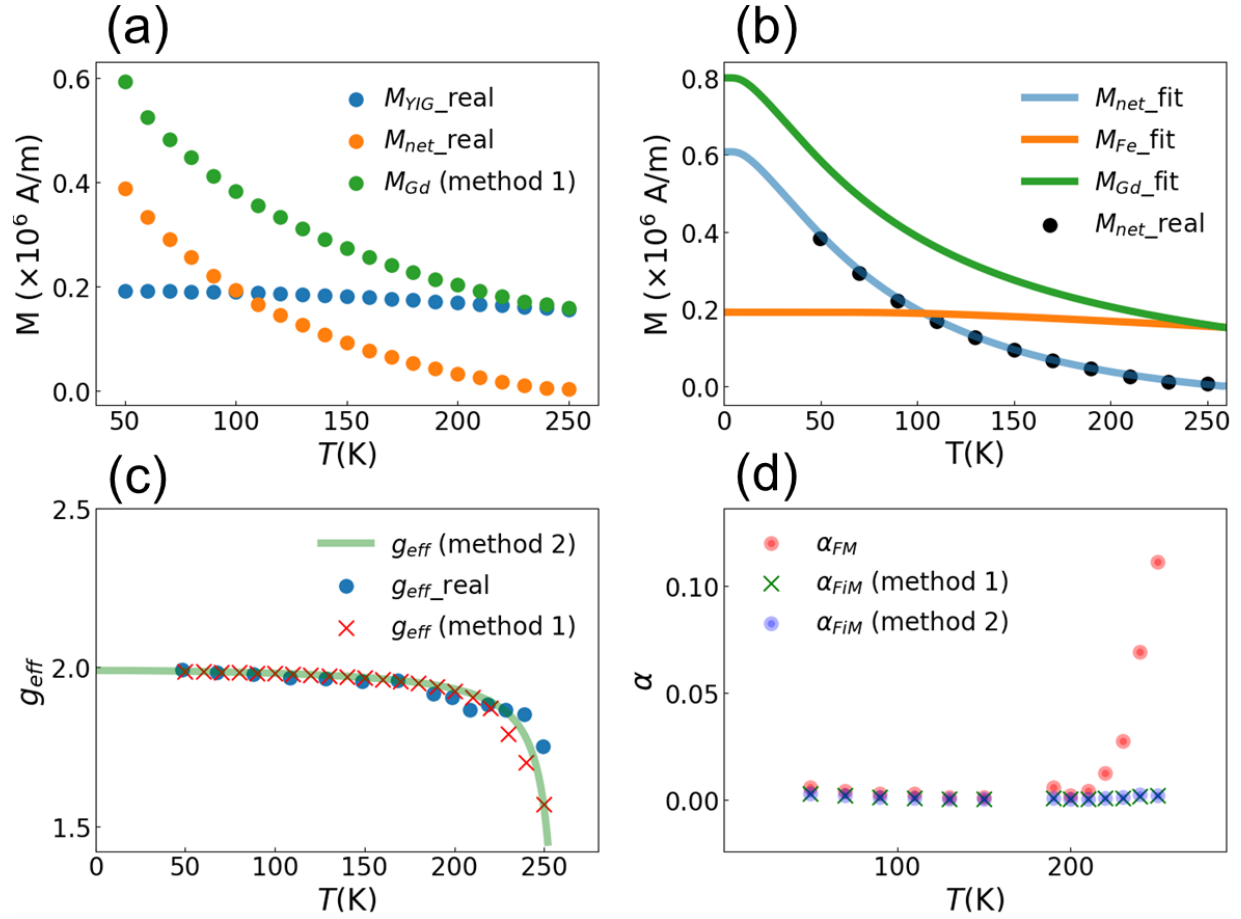


Figure 2. The analysis of GdIG data from Flaig *et al.*²⁶ (a) Calculated individual magnetization as a function of temperature using Method 1. (b) The Magnetization curve of GdIG using Brillouin fitting method (Method 2) compared to the magnetization from Flaig *et al.*²⁶ (c) The g_{eff} of GdIG calculated from Method 1 as the red cross and from Method 2 as the green line compared to the blue dot g_{eff} from Flaig *et al.*²⁶ (d) Comparing the damping parameter α_{FM} (red dot) to α_{FiM} based on Method 1 (green cross) and α_{FiM} based on Method 2 (blue dot).

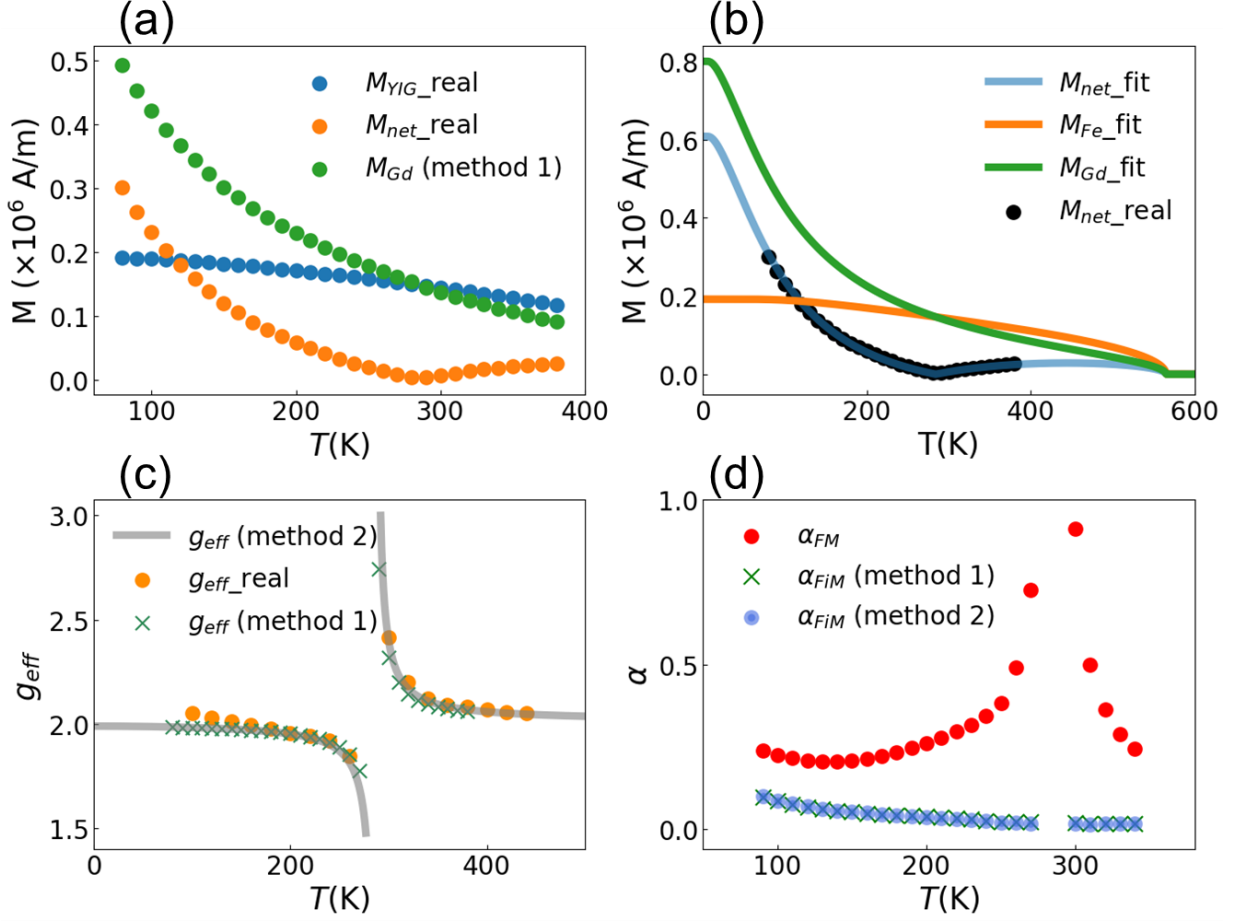


Figure 3. The analysis of GdIG data from Calhoun *et al.*^{19,20}. (a) Calculated individual magnetization as a function of temperature using Method 1. (b) The Magnetization curve of GdIG using Brillouin fitting method (Method 2) compared to the magnetization from Calhoun *et al.*²⁰ (c) The g_{eff} of GdIG calculated from Method 1 as the green cross and from Method 2 as the grey line compared to the yellow dot g_{eff} from Calhoun *et al.*¹⁹ (d) Comparing the damping parameter α_{FM} (red dot) to α_{FiM} based on Method 1 (green cross and α_{FiM} based on Method 2 (blue dot).

RESULTS AND DISCUSSIONS

We analyze three datasets and evaluate the validity of Method 1 and Method 2 using the formula provided above. The first dataset is from Rodrigue *et al.*²³, where the ΔH and g_{eff} in three directions [100], [110], [111] are provided. Note that the value of g_{eff} is calculated using the Kittel equation in Rodrigue's paper. The M_{net} is obtained from Dionne *et al.*¹⁸ where the GdIG has a similar compensation temperature to Rodrigue *et al.*²³. $f_{\text{res}}=9.165\text{GHz}$ and we assume that ΔH_0 is

zero since the GdIG is a polished sphere. We analyze the data using Method 1 and Method 2 and plot the results in Fig. 1. For Method 1, we can observe that the calculated temperature dependence of the M_{Gd} (see Fig. 1a) and the obtained g-factor (see Fig. 1c) are reasonable. Using Method 2, we get the fitting curves for magnetization from each sublattice and g-factor, which fit accurately to the experimental data.

The second dataset of the temperature dependence of FMR below the T_A is from Maier-Flaig *et al.*,²⁶ where the g-factor, ΔH , and M_{net} are also provided. Again, we can see that the magnetization as a function of temperature from two methods are in accordance with Flaig's data (see Fig. 2). g_{eff} calculated dots from Method 1 and fitting curves from Method 2 are highly consistent with the data, which illustrates that both two methods are well established.

The third set of data is from B. A. Calhoun *et al.*,^{19,20} where $f_{\text{res}} = 9.479\text{GHz}$. Similar results to the above two datasets are obtained as shown in Fig. 3.

To directly compare the above two methods, the ferrimagnetic damping parameter α_{FiM} calculated from these two methods are plotted against each other in Fig. 1, 2 and 3, using the data from Rodrigue *et al.*²³, Flaig *et al.*²⁶ and Calhoun *et al.*¹⁹. For all datasets, two different methods all give consistent results and have similar values: the newly defined damping parameter α_{FiM} of a ferrimagnetic material is not divergent near the T_A and has much lower value than α_{FM} . The α_{FiM} in all three datasets is at low value, revealing the achievability of fast domain-wall dynamics in ferrimagnetic insulator at the angular momentum compensation temperature.

CONCLUSION

In this work, we survey the literature dataset of FMR studies on the ferrimagnetic insulator GdIG and find that the ferrimagnetic damping parameter α_{FiM} does not increase when the temperature approaches the T_A , differing from the conventionally defined α_{FM} that shows divergence near the T_A . This validates the recently developed theory about damping in the ferrimagnetic systems and reveals that the damping parameter, when it is appropriately defined with no divergence at all temperatures, is not as high as previously thought. Our work suggests that analyzing the dynamics of ferrimagnets needs extra caution, that is not required for ferromagnets, in particular in the

vicinity of the T_A to avoid unphysical divergences. Besides, potentially lower damping in insulators suggests that ferrimagnetic insulators are promising for future ultrafast and ultralow-power spintronic applications.

ACKNOWLEDGEMENT

The authors at HKUST were supported by the Hong Kong Research Grants Council-Early Career Scheme (Grant No. 26200520) and the Research Fund of Guangdong-Hong Kong-Macao Joint Laboratory for Intelligent Micro-Nano Optoelectronic Technology (Grant No. 2020B1212030010). S.K.K. was supported by Brain Pool Plus Program through the National Research Foundation of Korea funded by the Ministry of Science and ICT (Grant No. NRF-2020H1D3A2A03099291) and by the National Research Foundation of Korea funded by the Korea Government via the SRC Center for Quantum Coherence in Condensed Matter (Grant No. NRF-2016R1A5A1008184).

REFERENCES

1. Jungwirth, T., Marti, X., Wadley, P. & Wunderlich, J. Antiferromagnetic spintronics. *Nature Nanotechnology* vol. 11 231–241 (2016).
2. Baltz, V. *et al.* Antiferromagnetic spintronics. *Rev. Mod. Phys.* **90**, (2018).
3. Finley, J. & Liu, L. Spin-Orbit-Torque Efficiency in Compensated Ferrimagnetic Cobalt-Terbium Alloys. *Phys. Rev. Appl.* **6**, (2016).
4. Caretta, L. *et al.* Fast current-driven domain walls and small skyrmions in a compensated ferrimagnet. *Nat Nanotechnol* (2018) doi:10.1038/s41565-018-0255-3.
5. Kim, K. J. *et al.* Fast domain wall motion in the vicinity of the angular momentum compensation temperature of ferrimagnets. *Nat Mater* **16**, 1187–1192 (2017).
6. Siddiqui, S. A., Han, J., Finley, J. T., Ross, C. A. & Liu, L. Current-Induced Domain Wall Motion in a Compensated Ferrimagnet. *Phys. Rev. Lett.* **121**, (2018).
7. Cai, K. *et al.* Ultrafast and energy-efficient spin-orbit torque switching in compensated ferrimagnets. *Nat. Electron.* **3**, 37–42 (2020).

8. Stanciu, C. D. *et al.* Ultrafast spin dynamics across compensation points in ferrimagnetic GdFeCo: The role of angular momentum compensation. *Phys. Rev. B - Condens. Matter Mater. Phys.* **73**, (2006).
9. Okuno, T. *et al.* Temperature dependence of magnetic resonance in ferrimagnetic GdFeCo alloys. *Appl. Phys. Express* **12**, (2019).
10. Kim, D.-H. *et al.* Low Magnetic Damping of Ferrimagnetic GdFeCo Alloys. *Phys. Rev. Lett.* **122**, 127203 (2019).
11. Kamra, A., Troncoso, R. E., Belzig, W. & Brataas, A. Gilbert damping phenomenology for two-sublattice magnets. (2018) doi:10.1103/PhysRevB.98.184402.
12. Shao, Q. *et al.* Role of dimensional crossover on spin-orbit torque efficiency in magnetic insulator thin films. *Nat. Commun.* **9**, 3612 (2018).
13. Avci, C. O. *et al.* Current-induced switching in a magnetic insulator. *Nat. Mater.* **16**, 309–314 (2017).
14. Avci, C. O. *et al.* Interface-driven chiral magnetism and current-driven domain walls in insulating magnetic garnets. *Nat. Nanotechnol.* **14**, 561–566 (2019).
15. Shao, Q. *et al.* Topological Hall effect at above room temperature in heterostructures composed of a magnetic insulator and a heavy metal. *Nat. Electron.* **2**, 182–186 (2019).
16. Li, P. *et al.* Spin-orbit torque-assisted switching in magnetic insulator thin films with perpendicular magnetic anisotropy. *Nat. Commun.* **7**, 12688 (2016).
17. Boyd, E. L., Moruzzi, V. L. & Smart, J. S. Sublattice Magnetizations in Rare-Earth Iron Garnets. *J. Appl. Phys.* **34**, 3049–3054 (1963).
18. Dionne, G. F. Molecular field and exchange constants of Gd³⁺-substituted ferrimagnetic garnets. *J. Appl. Phys.* **42**, 2142–2143 (1971).
19. Calhoun, B. A., Overmeyer, J. & Smith, W. V. Ferrimagnetic Resonance in Gadolinium Iron Garnet. *Phys. Rev.* **107**, 993–994 (1957).
20. Calhoun, B. A., Smith, W. V. & Overmeyer, J. Ferrimagnetic resonance in gadolinium iron garnet. *J. Appl. Phys.* **29**, 427–428 (1958).
21. Geller, S., Remeika, J. P., Sherwood, R. C., Williams, H. J. & Espinosa, G. P. Magnetic Study of the Heavier Rare-Earth Iron Garnets. *Phys. Rev.* **137**, A1034–A1038 (1965).
22. Geschwind, S. Sign of the ground-state cubic crystal field splitting parameter in Fe³⁺. *Phys. Rev. Lett.* **3**, 207–209 (1959).

23. Rodrigue, G. P., Meyer, H. & Jones, R. V. Resonance measurements in magnetic garnets. *J. Appl. Phys.* (1960) doi:10.1063/1.1984756.
24. Coey, J. M. D. *Magnetism and magnetic materials. Magnetism and Magnetic Materials* vol. 9780521816144 (Cambridge University Press, 2010).
25. Espinosa, G. P. Crystal chemical study of the rare-earth iron garnets. *J. Chem. Phys.* **37**, 2344–2347 (1962).
26. Maier-Flaig, H. *et al.* Perpendicular magnetic anisotropy in insulating ferrimagnetic gadolinium iron garnet thin films. (2017).
27. Caretta, L. *et al.* Relativistic kinematics of a magnetic soliton. *Science (80-.)*. **370**, 1438–1442 (2020).
28. Zhou, H.-A. *et al.* Compensated magnetic insulators for extremely fast spin-orbitronics. 1–17 (2019).